Wideband optical vector network analyzer based on optical single-sideband modulation and optical frequency comb

Min Xue, Shilong Pan,* Chao He, Ronghui Guo, and Yongjiu Zhao

Key Laboratory of Radar Imaging and Microwave Photonics (Nanjing Univ. Aeronaut. Astronaut.),
Ministry of Education Nanjing University of Aeronautics and Astronautics, Nanjing 210016, China
*Corresponding author: pans@ieee.org

A novel approach to increase the measurement range of the optical vector network analyzer (OVNA) based on optical single-sideband (OSSB) modulation is proposed and experimentally demonstrated. In the proposed system, each comb line in an optical frequency comb (OFC) is selected by an optical filter and used as the optical carrier for the OSSB-based OVNA. The frequency responses of an optical device-under-test (ODUT) are thus measured channel by channel. Because the comb lines in the OFC have fixed frequency spacing, by fitting the responses measured in all channels together, the magnitude and phase responses of the ODUT can be accurately achieved in a large range. A proof-of-concept experiment is performed. A measurement range of 105 GHz and a resolution of 1 MHz is achieved when a five-comb-line OFC with a frequency spacing of 20 GHz is applied to measure the magnitude and phase responses of a fiber Bragg grating.   © 2013 Optical Society of America

OCIS codes: (300.0300) Spectroscopy; (300.6320) Spectroscopy, high-resolution; (300.6370) Spectroscopy, microwave; (300.6380) Spectroscopy, modulation.
http://dx.doi.org/10.1364/OL.38.004900

As the rapid development of the high-capacity optical communications, it is essential to increase the spectral efficiency by finely manipulating the optical spectrum. A large number of optical devices with the capability of processing optical signals with extremely high resolution were reported, such as optical ring resonators [1], optical whispering-gallery mode resonators [2], and ultra-narrow fiber Bragg gratings (FBGs) [3]. However, the detailed frequency responses of such devices, especially the phase responses, cannot be easily measured using the commercially available optical spectrum analyzers (OSAs). Thus, an optical vector network analyzer (OVNA), which can measure simultaneously the magnitude and phase responses of an optical device-under-test (ODUT) with high resolution, is highly desired. Previously, the OVNA was realized using the modulation phase-shifted method [4] or interferometry approach [5]. However, both of these methods rely on the wavelength scan of the laser source, so that the resolution could not be high (typically >1 pm or 125 MHz) due to the low wavelength accuracy and poor wavelength stability of the state-of-the-art wavelength-swept laser source. To solve this problem, an OVNA based on optical single-sideband (OSSB) modulation was proposed [6–13]. The measurement resolution of the OSSB-based OVNA can reach 78 kHz in experiment [11] and several hertz in theory [6]. However, the measurement range of the OVNA is limited (less than 40 GHz) due to the small bandwidth of the electro-optic devices. Although applying a tunable laser source (TLS) might help to extend the measurement range, the measurement resolution of the OVNA would again be restricted by the low wavelength accuracy and poor wavelength stability of the TLS.

In this Letter, we propose, for the first time to the best of our knowledge, a novel approach to boost the measurement range of the OSSB-based OVNA. In the proposed approach, a series of optical carriers with fixed

frequency spacing are provided by an optical frequency comb (OFC) together with a tunable optical bandpass filter (TOBPF). As the magnitude and phase responses measurement in a certain range is achieved with each carrier, the measurement range of the OSSB-based OVNA can be extended by about n times if an n-comb-line OFC is applied. A proof-of-concept experiment is carried out. When a five-comb-line OFC with a frequency spacing of 20 GHz is used, a measurement range as large as 105 GHz and a resolution of 1 MHz are achieved.

The schematic diagram of the proposed approach to extend the measurement range of the OSSB-based OVNA is shown in Fig. 1. The system consists of two key parts, i.e., an OFC-based optical carrier generator and an OSSB-based OVNA. In the OFC-based optical carrier generator,
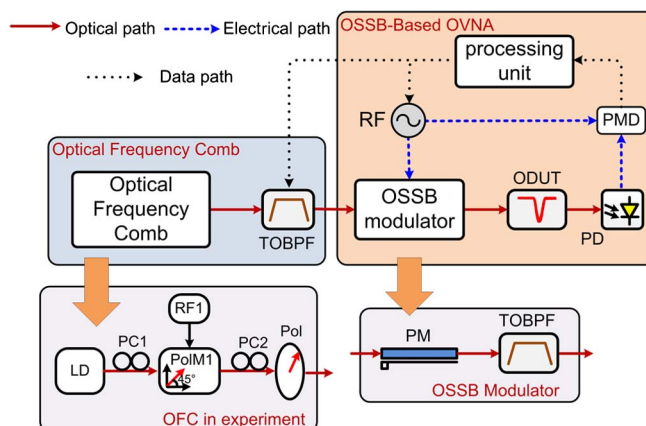

Fig. 1.   Schematic diagram of the proposed approach to extend the measurement range of the OSSB-based OVNA. LD, laser diode; PC, polarization controller; PolM, polarization modulator; RF, radio frequency; Pol, polarizer; TOBPF, tunable optical bandpass filter; PM, phase modulator; FBG, fiber Bragg grating; PD, photodetector; PMD, phase-magnitude detector.

a series of optical carriers with fixed frequency spacing are generated by an OFC. A TOBPF is followed to select one comb line from the OFC. Then, the selected comb line is served as the optical carrier for the OSSB-based OVNA to measure the frequency responses of the ODUT in the corresponding channel. In the OSSB-based OVNA, the comb line from the OFC-based optical carrier generator is modulated by a RF signal at an OSSB modulator. Then, the OSSB signal is sent to the ODUT. In the ODUT, the phase and magnitude of the optical carrier and sideband in the OSSB signal would be changed according to the transmission response of the ODUT. After the square-law detection in the photodetector (PD), the phase and magnitude of the electrical component with the same frequency of the driven RF signal are extracted by a phase-magnitude detector and compared with those of the driven RF signal. By scanning the frequency of the RF signal, corresponding to the scan of the wavelength of the sideband in the OSSB signal, the frequency responses of the ODUT in the corresponding channel are obtained [12]. Similarly, the frequency responses of the ODUT in the other channels can be obtained. Thanks to the fixed frequency spacing of the OFC, the responses in the adjacent channels can be fitted together. The influence of the amplitude and phase difference between the comb lines can be eliminated by the continuity of the frequency response of the ODUT in the boundary of two consecutive channels. From the above principle, if an n-comb-line OFC is employed, the frequency responses of the ODUT in the range of $(n-1) \times \Delta\omega + \Delta\omega_e$ can be measured, where $\Delta\omega$ and $\Delta\omega_e$ are the frequency spacing of the OFC and the measurement range of the single-channel OSSB-based OVNA, respectively. $\Delta\omega$ must be smaller than or equal to $\Delta\omega_e$, so that the responses in the adjacent channels can be fit together.

A proof-of-concept experiment based on the setup shown in Fig. 1 is carried out. In the OFC-based optical carrier generator, a light wave with a power of 16 dBm from a TLS (Agilent N7714A) is modulated by a RF signal at a polarization modulator (PolM). The PolM has a bandwidth of 40 GHz and a half-wave voltage of 3.5 V at 1 GHz (Versawave Inc.). The frequency of the RF signal is 20 GHz, which is generated by a vector signal generator (Agilent E8267D). A RF power amplifier (Agilent 83020A) is used to amplify the RF signal to a satisfactory power level. By adjusting two polarization controllers placed before and after the PolM, a flat five-comb-line OFC with fixed frequency spacing is generated at the output of a polarizer [14]. Then, a TOBPF (Finisar Wave-Shaper4000s) with a narrow passband is used to select one comb line from the OFC. In the OSSB-based OVNA, a 50 GHz electrical vector network analyzer (EVNA, Agilent N5245A) is used to serve as both a tunable RF source and a phase-magnitude detector. The selected comb line is modulated by the RF signal from the EVNA at an OSSB modulator. The OSSB modulator consists of a 40 GHz phase modulator (OESPACE Inc.) and another TOBPF (Yenista XTM-50) with an edge slope of about 500 dB/nm, by which one sideband of the phase-modulated signal is removed. A 50 GHz PD with a responsivity of 0.65 A/W is employed to convert the optical signal to an electrical signal, which is then received and processed by the EVNA. The optical spectra

are obtained by an OSA (Yokogawa AQ6370C) with a resolution of 0.02 nm.

Figure 2(a) shows the optical spectra of the five-comb-line OFC with a frequency spacing of 20 GHz generated by the PolM together with the polarizer. As can be seen, five flat spectral lines, which have a power variation within 0.4 dB, a wavelength spacing of 0.16 nm (or 20 GHz), and an unwanted-mode suppression ratio of 13.092 dB are obtained. With the help of the TOBPF, each comb line is selected, as shown in Fig. 2(b). Due to the wavelength-dependent insertion loss variation of the TOBPF, the power variation of the five selected optical carriers is deteriorated to be 1.733 dB. In addition, the sidemode in each channel is suppressed to be less than −39 dBc.

Figure 3 shows the magnitude and phase responses of an FBG measured by the proposed approach in a range of 105 GHz. Applying the five optical carriers, the magnitude and phase responses of the FBG in five consecutive channels are measured. In each channel, the measurement resolution is 1 MHz and the measurement range is 25 GHz (10–35 GHz offset the carrier). Since the channel spacing is 20 GHz, there is 5 GHz overlapped areas between every two adjacent channels (the shadows in Fig. 3). For instance, the shadow between channel 1 and channel 2 is the overlap of the measurement area between 30 and 35 GHz away from the optical carrier in channel 1 and that between 10 and 15 GHz away from the optical carrier in channel 2. Thanks to the fixed frequency spacing of the adjacent optical carriers, the overlapped curves are well superimposed, as shown in the
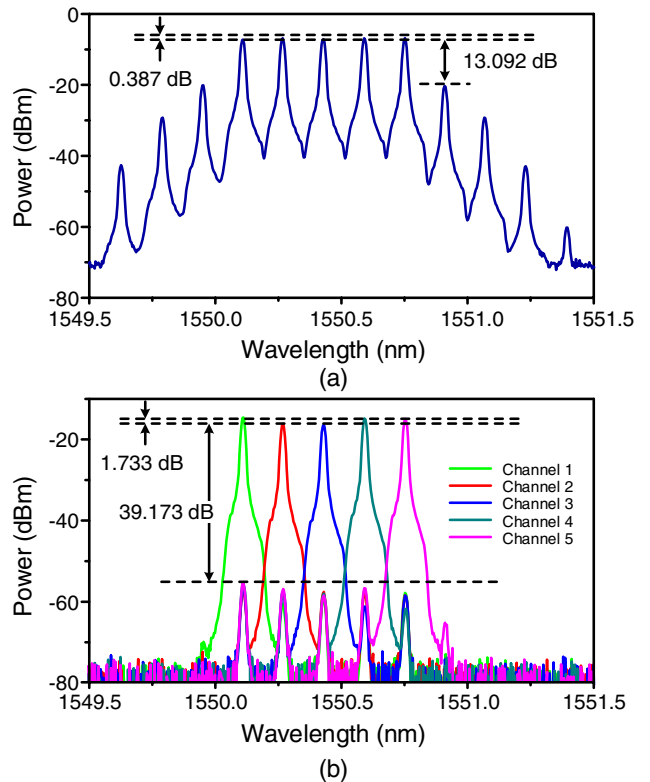

Fig. 2.   Optical spectra of (a) the five-comb-line OFC with a frequency spacing of 20 GHz and (b) the five optical carriers selected from the OFC by the TOBPF.
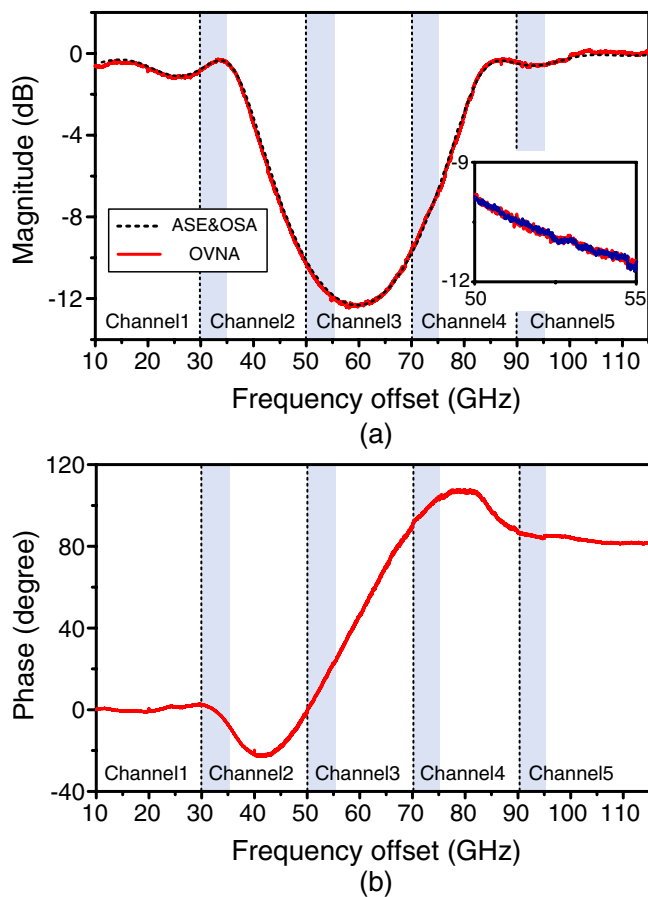
Fig. 3.   (a) Magnitude and (b) phase responses of a FBG measured by the proposed approach in the range of 105 GHz.

In conclusion, a novel approach to extend the measurement range of the OSSB-based OVNA using an OFC was proposed and demonstrated. By applying an OFC with five comb lines and 20 GHz frequency spacing in the proof-of-concept experiment, the magnitude and phase responses of the FBG in the range of 105 GHz was achieved with a resolution of 1 MHz. The proposed method can find application in high-spectral-efficiency optical communications, high-precision optical sensors, high-accuracy optical metrology, and photonic integrated circuits.

inset of Fig. 3(a). In the overlapped area, an algorithm is used to maintain the continuity of the responses of the FBG in the two channels, so that the responses measured in adjacent channels can be fitted together. To verify measurement results, the magnitude response of the FBG is also measured by using an amplified spontaneous emission source together with an OSA. As can be seen from Fig. 3(a), the two curves are well superimposed.

Based on the proposed approach, a much larger measurement range can be achieved if an OFC with more comb lines and broader frequency spacing is used [15]. The measurement resolution can also be increased if a frequency-swept RF source with high resolution is applied. The measurement can be accelerated if dense wavelength division multiplexing technology and parallel measurement are used. It should be noted that for broad OFCs, the optical power for each comb line is very low. To solve this problem, an optical amplifier can be inserted to amplify the power of the selected comb line to a satisfying level.

References

1. J. Riemensberger, K. Hartinger, T. Herr, V. Brasch, R. Holzwarth, and T. J. Kippenberg, Opt. Express **20**, 27661 (2012).
2. I. Fescenko, J. Alnis, A. Schliesser, C. Y. Wang, T. J. Kippenberg, and T. W. Hänsch, Opt. Express **20**, 19185 (2012).
3. Y. Painchaud, M. Aubé, G. Brochu, and M.-J. Picard, *Bragg Gratings, Photosensitivity, and Poling in Glass Waveguides*, OSA Technical Digest (CD) (Optical Society of America, 2010), paper BTuC3.
4. T. Niemi, M. Uusimaa, and H. Ludvigsen, IEEE Photon. Technol. Lett. **13**, 1334 (2001).
5. G. D. Van Wiggeren, A. R. Motamedi, and D. M. Baney, IEEE Photon. Technol. Lett. **15**, 263 (2003).
6. J. E. Román, M. Y. Frankel, and R. D. Esman, Opt. Lett. **23**, 939 (1998).
7. R. Hernandez, A. Loayssa, and D. Benito, Opt. Eng. **43**, 2418 (2004).
8. A. Loayssa, R. Hernández, D. Benito, and S. Galech, Opt. Lett. **29**, 638 (2004).
9. M. Sagues and A. Loayssa, Electron. Lett. **47**, 47 (2011).
10. M. Sagues and A. Loayssa, Opt. Express **18**, 17555 (2010).
11. Z. Z. Tang, S. L. Pan, and J. P. Yao, Opt. Express **20**, 6555 (2012).
12. M. Xue, S. L. Pan, X. W. Gu, and Y. J. Zhao, J. Opt. Soc. Am. B **30**, 928 (2013).
13. M. Wang and J. P. Yao, IEEE Photon. Technol. Lett. **25**, 753 (2013).
14. C. He, S. L. Pan, R. H. Guo, Y. J. Zhao, and M. H. Pan, Opt. Lett. **37**, 3834 (2012).
15. I. S. Grudinin, L. Baumgartel, and N. Yu, Opt. Express **20**, 6604 (2012).